Chinese Herbal Medicines 11 (2019) 185–191

Contents lists available at ScienceDirect

Chinese Herbal Medicines

journal homepage: www.elsevier.com/locate/chmed

Original Article

Metabolic profiling of icaritin in rats using UHPLC-Q/TOF-MS

Tong Wang[a,b,1], Xin-chi Feng[a,1], Li-qin Ding[b], Kun Wang[a,b], Xu-liu Shi[a,b], Li-wei Chai[a,b], Yang Li[a,b], Feng Qiu[a,b,*]

[a] School of Chinese Materia Medica, Tianjin University of Traditional Chinese Medicine, Tianjin 300193, China
[b] Tianjin State Key Laboratory of Modern Chinese Medicine, Tianjin University of Traditional Chinese Medicine, Tianjin 300193, China

ARTICLE INFO

Article history:
Received 14 May 2018
Revised 30 May 2018
Accepted 21 November 2018
Available online 21 March 2019

Keywords:
icaritin
metabolites
Metabolynx
rats
UHPLC/Q-TOF-MS/MS

ABSTRACT

Objective: To identify the *in vivo* metabolites of icaritin and speculate its metabolic profiling in rats.
Methods: The plasma, bile, urine, and feces of rats were collected after orally administration of icaritin at a dose of 100 mg/kg and detected by an ultra-high performance liquid chromatography coupled with quadrupole time-of-flight mass spectrometry (UPLC/Q-TOF-MS/MS) in both positive and negative modes. The data of treated and control groups were compared and analyzed with the aid of Metabolynx XS software.
Results: A total of 25 metabolites were identified in the biosamples, and 14 of them were reported for the first time to our knowledge.
Conclusion: The main metabolite types of icaritin in rats were glucuronide conjugation, methylation, hydroxylation, reduction, and acetylation.

1. Introduction

Epimedii Folium, the dried leaves of *Epimedium brevicornu* Maxim., *Epimedium sagittatum* (Sieb. et Zucc.) Maxim., *Epimedium pubescens* Maxim., and *Epimedium koreanum* Nakai, is one of the most commonly used medicine for kidney disease and rheumatism (Wang, Yuan, Li, & Zhang, 2017), and flavonoids from the plants of *Epimedium* L. have a wider range of pharmacological effects than other ingredients (Jiang, Zhao, Song, & Jia, 2016a). As the intestinal metabolite (Yao et al., 2012) and one of the main active compounds of *Epimedium* (Wang et al., 2013), icaritin (Fig. 1) is extensively researched owing to its comprehensive therapeutic effects, such as anti-osteoporosis (Tan, Li, Indran, Chew, & Yong, 2017; Wu et al., 2017), anticancer (Li et al., 2013; Sun et al., 2016; Xu et al., 2015), antidiabetic (Kim, Jung, Sohn, Kim, & Choi, 2017), neuroprotective effect (Jiang, Chen, Zhao, Zhang, & Chen, 2016b; Sun et al., 2018), and improvement of liver fibrosis (Li et al., 2011). Despite the outstanding pharmacological activities and the bioavailability of icaritin were poor (Liu et al., 2010), which enlightened us that the metabolites of icaritin might be responsible for various pharmacological activities.

Owing to the high background noise and complicated metabolic types, detecting the drug-related metabolites *in vivo* was a challenging task all along until the ultra-high performance liquid chromatography coupled with mass spectrometry (UHPLC-MS/MS) was applied in this field (Feng et al., 2017). With the excellent sensitivity, accuracy and comprehensive nature of metabolites detection, quadrupole time-of-flight (TOF) analyzer is more suitable for the study on the metabolism compared with other MS detectors.

To date, several articles are available concerning the metabolism of icaritin (Jiang et al., 2014; Ye et al., 2015; Zhang et al., 2017; Zhang & Zhang, 2017). While, most of these studies focused on metabolites in urine and plasma, and more attention was paid to the Phase II metabolism. To make the metabolism fates of icaritin more comprehensive, a test and analysis method was established with the aid of an ultra-high performance liquid chromatography coupled with quadrupole time-of-flight mass spectrometry (UHPLC/Q-TOF-MS/MS) and the Metabolynx XS software via setting a variety of reaction types to make the results more accurate and convictive which will give in-depth insights of the metabolism of icaritin.

2. Materials and methods

2.1. Chemicals and reagents

Leucine-encephalin and formic acid were purchased from Sigma-Aldrich (Poole, UK). LC/MS-grade methanol and acetonitrile were purchased from Fisher Scientific (USA). Deionized water and

* Corresponding author.
E-mail address: fengqiu20070118@163.com (F. Qiu).
[1] These authors contributed equally to this work.

https://doi.org/10.1016/j.chmed.2019.03.008
1674-6384/

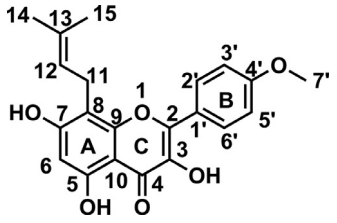

Fig. 1. Structure of icaritin.

pure water was purified using a Milli-Q system (Millipore, USA). Icaritin was purchased from Shanghai Yuanye Bio-Technology Co., Ltd. (Shanghai, China). All other reagents were of analytical grade.

2.2. Animals

Twenty-seven healthy SPF male Sprague-Dawley (SD) rats (200 ± 20) g were purchased from the Experimental Animal Centre, Academy of Military Medical Sciences (Beijing, China). All animals were allowed water and standard chow *ad libitum* and acclimatized to the facilities for one week. All the rats were fasted with free access to water for a period of 12 h prior to the experiment.

2.3. Instrumentation and conditions

UHPLC was performed using an ACQUITY^{TM} UPLC I-Class system equipped with a binary solvent system and an auto-sampler. Chromatographic separation was performed on an ACQUITY UPLC BEH Shield RP_{18} column (2.1 × 50 mm, 1.7 µm) held at 40 °C, and the flow rate was 0.4 mL/ min. The mobile phase consisted of water (A) and acetonitrile (B), both containing 0.1% formic acid, was delivered using a linear gradient program as follows: 5%–8% B from 0 to 3 min, 8%–25% B from 3 to 10 min, 25%–50% B from 10 to 20 min, 50%–100% B from 20 to 25 min.

Mass spectrometry detection was performed using a Waters Xevo G2-S UPLC-Q/TOF-MS (Waters, Milford, USA) equipped with an electrospray ion source operating in positive and negative ion modes. The optimal conditions of analysis were employed as follows: The sampling cone voltage was 30 V; The capillary voltage was 2.5 kV in positive and negative ion mode; The source temperature was set at 100 °C; The extraction cone voltage was 3.0 V; The desolvation temperature was set at 400 °C; The cone gas flow was 50 L/h; And the desolvation gas flow was 800 L/h. In MS^E mode, the trap collision energy of the low-energy and high-energy function was set at 0 eV and 10–50 eV, respectively. In MS^2 mode, the collision energy was set at 25 eV. Data were in centroid mode from 50 to 1200 Da. For accurate mass acquisition, the mass was corrected using leucine-encephalin via a LockSpray^{TM} interface at a flow rate of 5 µL/min, monitoring a reference ion for positive ion mode ($[M+H]^+ = 556.2771$) and negative ion mode ($[M-H]^- = 554.2615$) to ensure accuracy during MS analysis.

2.4. Data processing software

All data were acquired and processed with Metabolynx software under the operating interface of Masslynx V4.1 (Waters, Milford, MA, USA). The parameter settings were as follows: the analysis time was 0–25 min; The mass window was 0.1 Da; The absolute area of the peak was 50 (p.a.u.); The mass defect filter was set at ± 40 mDa; The maximum tolerance of mass error was set as 5 × 10^{-6}; The spectrum was above the relative intensity of 2%; And the degree of unsaturation was set in a range from 6 to 15. The prediction rules of elemental composition were defined as follows: atom numbers of carbon, hydrogen, oxygen, nitrogen, and sulfur were set to ranges of 0–40, 0–50, 0–25, 0–5, and 0–5, respectively. Blank biological samples were used as controls for comparison with the analytic samples, and they were all processed under the same conditions.

2.5. Sample collection

As icaritin is the main constituent of *E. brevicomu* which is taken with course of treatment in the traditional use of Chinese medicine, the three consecutive days of orally administration was conducted in this study. And the rats were divided into three groups in view of the individual difference among them. All rats were orally administrated with icaritin at the dose of 100 mg/kg (0.5% CMC-Na in water as vehicle) per day.

For the collection of feces and urine samples, three rats were maintained in metabolic cages separately and orally administrated with icaritin for three consecutive days. Then the feces and urine were collected during the following 72 h.

Three rats were anesthetized by intraperitoneal injection of 1 mL 20% ethyl carbamate after drug treatment for three consecutive days and the bile duct cannulation was operated for the collection of bile. Then the wound was sutured and a heating lamp was used to maintain the body temperature of rats. Bile samples were collected for 48 h.

In consideration of the fact that the metabolites were produced with time, it was considered more rigorous to collect blood at different time after oral administration. Twelve rats were dosed for three consecutive days and divided into four groups randomly. Then, a cervical incision was made to collect the whole blood from the carotid artery at 1, 6, 12, and 24 h respectively after anesthetized by intraperitoneal injection of 1 mL 20% ethyl carbamate. The blood was centrifuged at 8000 r/min for 10 min at 4 °C to obtain the plasma.

Blank samples were collected following the same protocol from nine rats (three rats for the collection of blank bile, three for blank plasma and three for blank urine and feces) in control group after orally administrated with vehicle (0.5% CMC-Na) for three consecutive days.

2.6. Sample preparation

To make the results as comprehensive as possible, the same biosamples of each rat were mixed uniformly after collection. An aliquot of 2 mL of urine sample and 1 mL bile sample were loaded onto ODS columns (500 mg) which were preconditioned and equilibrated with methanol and water respectively, and then the cartridges were eluted with 5 mL of methanol and evaporated to dryness under nitrogen gas at room temperature. The obtained residues of urine and bile samples were reconstituted in 400 µL and 200 µL acetonitrile-water (1:1, volume ratio), respectively.

750 µL plasma sample was extracted by 2.5 mL acetonitrile and then vortexed for 5 min to precipitate protein. After centrifugation at 14 000 rpm for 10 min, the supernatant was transferred into a clean tube and dried under nitrogen gas at room temperature. The residue was reconstituted in 750 µL acetonitrile-water (1:1, volume ratio).

The feces samples were freeze-dried and pulverized into fine powder. The thorough mixed powder was immersed in methanol (1:10, mass-to-volume ratio) and ultrasonically extracted for 30 min at room temperature. The extracted solution was centrifuged at 8000 rpm for 10 min to get the supernatant which was evaporated to dryness under nitrogen gas at room temperature later. Finally, the residue was reconstituted in 300 µL acetonitrile-water (1:1, volume ratio).

3. Results

A total of 25 metabolites (**M1**–**M25**) were identified in this study, and their extracted mass chromatograms were illustrated in Fig. 2 and Table 1.

3.1. Phase II metabolites of icaritin

M1 ($C_{33}H_{36}O_{18}$) was eluted at 5.00 min with the deprotonated ion at 719.1820. The typical neutral loss of 176 Da (gluA) between the ions at *m/z* 719.1820 and 543.1506 and another one between the ions at *m/z* 543.1506 and 367.1180 indicated that the two molecules of glucuronide conjugation occurred, while the positions remain uncertain.

M2 ($C_{21}H_{20}O_{10}S$) was diagnosed as a sulfated metabolite by reason of the typical neutral loss of 80 Da (SO_3) between the deprotonated ion at *m/z* 463.0699 and its fragment ion at *m/z* 383.1142. Based on the elemental composition of fragment ions at *m/z* 383.1142 ($C_{21}H_{19}O_7$) and 353.1031 ($C_{20}H_{17}O_6$) recommended by Metabolynx software, there was a neutral loss of 30 Da (CH_2O) with the unchanged degree of unsaturation. Thus, it was speculated that besides the sulfation at certain inconclusive position, the epoxidation occurred at the isopentenyl and the demethylation occurred at B-ring.

With the molecular ion at *m/z* 545.1654, 176 Da more than that of **M0**, **M6** ($C_{27}H_{28}O_{12}$) was diagnosed as the mono-glucuronide conjugation of icaritin, while, the exact reactive site was uncertain.

3.2. Hydroxylation and epoxidation metabolites of icaritin

M3 and **M16** shared the same formula ($C_{21}H_{20}O_8$) and molecular ion at 401.1231 which was 32 Da (2O) more than that of M0. Based on the MS/MS spectrum of M3, the neutral loss of 18 Da (H_2O) between the ions *m/z* 401.1231 and 383.1125 and another one between the ions at *m/z* 355.1160 and 337.1078 indicated that M3 should be the dihydroxylation product of icaritin, but the position of hydroxyls remained inconclusive. Only one neutral loss of 18 Da (H_2O) was detected in the MS/MS spectrum of M16 between its molecular ion and fragment ion at *m/z* 383.1129, which suggested that the hydroxylation occurred at least once. The fragment

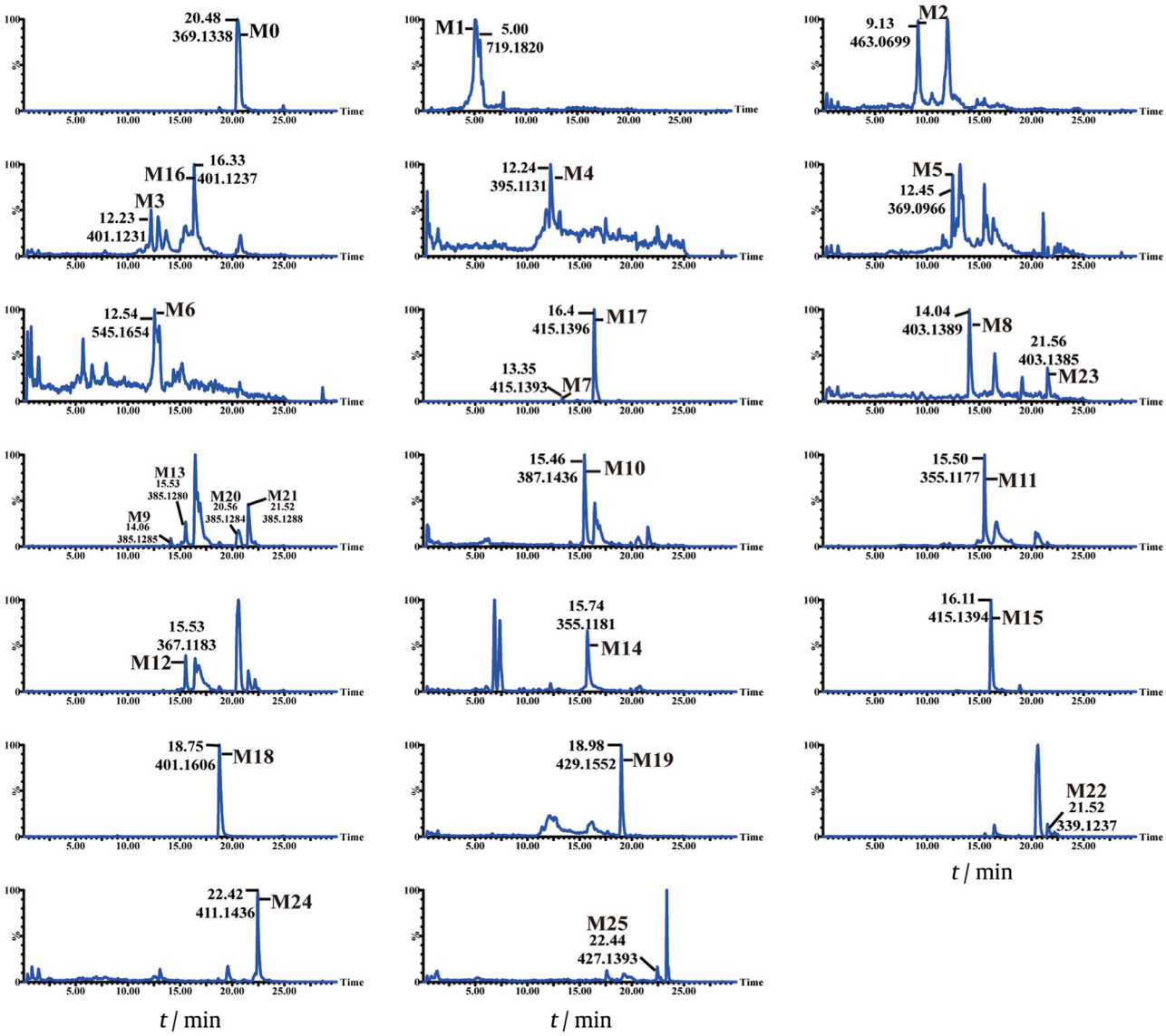

Fig. 2. ESI extracted ion chromatograms (BPI) of icaritin and its metabolites.

Table 1
UPLC-Q-TOF-MS retention times and fragment ions of metabolites of icaritin in rats.

No.	t_R /min	Formula	Molecular ions $[M+H]^+$		$\times 10^{-6}$	Molecular ions $[M-H]^-$		$\times 10^{-6}$	MS/MS fragment	Metabolite description	F	U	B	P
			Cal.	Mea.		Cal.	Mea.							
M1#	5.00	$C_{33}H_{36}O_{18}$	721.198	721.1986	0.8	719.1823	719.182	−0.4	367.1180;543.1506	2Glucuronide conjugation	-	-	+	+
M2#	9.13	$C_{21}H_{20}O_{10}S$	465.0855	-	-	463.0699	463.0699	0	353.1031;383.1142	Sulfation + Epoxidation	+	-	-	-
M3	12.23	$C_{21}H_{20}O_8$	401.1236	401.1231	−1.2	399.108	399.1081	0.3	135.0466; 325.1054; 337.1078; 355.1160; 383.1125	2Hydroxylation	+	-	+	-
M4	12.24	$C_{22}H_{18}O_7$	395.1131	395.1124	−1.8	393.0974	393.0972	−0.5	135.0448; 297.0782; 325.0715	Acetylation + Demethylation + Dehydrogenation	+	-	-	-
M5#	12.45	$C_{20}H_{18}O_7$	371.1131	-	-	369.0974	369.0966	−2.2	219.0669; 325.1075; 353.1033	Epoxidation + Demethylation	+	-	-	-
M6	12.54	$C_{27}H_{28}O_{12}$	545.1659	545.1654	−0.9	543.1503	543.152	3.1	313.0717; 369.1344	Glucuronide conjugation	+	+	+	+
M7#	13.35	$C_{22}H_{24}O_8$	417.1549	417.1535	−3.4	415.1393	415.1386	−1.7	151.0392; 263.0916; 311.0573; 329.1411; 343.1532; 355.1182; 359.1499; 365.1017; 387.1453	2Reduction + Hydroxylation + Methylation + Oxidation	+	-	-	-
M8	14.04	$C_{21}H_{22}O_8$	403.1393	403.1389	−1	401.1236	401.1232	−1	135.0465; 313.0718; 367.1152; 385.1293	2Hydroxylation + Reduction	+	+	-	-
M9	14.06	$C_{21}H_{20}O_7$	385.1287	385.1285	−0.5	383.1131	-	-	135.0465; 285.0761; 329.0646; 339.1216; 367.1182	Hydroxylation	+	-	-	-
M10	15.46	$C_{21}H_{22}O_7$	387.1444	387.1436	−2.1	385.1287	385.1287	0	135.0467; 313.0714; 369.1335	Hydroxylation + Reduction	+	-	-	-
M11#	15.5	$C_{20}H_{20}O_6$	357.1338	-	-	355.1182	355.1177	−1.4	311.1288; 327.1232	Reduction + Hydroxylation	+	-	-	-
M12	15.53	$C_{21}H_{18}O_6$	367.1182	367.1183	0.3	365.1025	365.1025	−0.8	135.0463; 283.0607; 311.0563; 339.1225	Dehydrogenation	+	+	-	-
M13	15.53	$C_{21}H_{20}O_7$	385.1287	385.128	−1.8	383.1131	383.1137	1.6	135.0462; 283.0618; 311.0554; 339.1233; 367.1189	Hydroxylation	+	+	-	-
M14	15.74	$C_{20}H_{18}O_6$	355.1182	355.1181	−0.3	353.1025	353.1022	−0.8	299.0549	Demethylation	+	-	-	-
M15	16.11	$C_{22}H_{22}O_8$	415.1393	415.1394	0.2	413.1236	413.123	−1.5	135.0459; 313.0717; 357.0960; 383.1099	Hydroxylation + Reduction + Oxidation + Methylation	+	-	-	-
M16	16.33	$C_{21}H_{20}O_8$	401.1236	401.1237	0.2	399.108	399.1076	−1	135.0464; 313.0729; 355.1187; 383.1129	2Hydroxylation	+	-	-	-
M17#	16.4	$C_{22}H_{24}O_8$	417.1549	417.1545	−1	415.1393	415.1396	0.7	311.0537; 323.0547; 367.1163; 383.1162; 397.1292	2Hydroxylation + Reduction + Methylation	+	-	-	-
M18	18.75	$C_{22}H_{24}O_7$	401.16	401.1606	1.5	399.1444	399.1438	−1.5	313.0707; 369.1331; 401.1586	Hydroxylation + Methylation + Reduction	+	-	-	-
M19	18.98	$C_{23}H_{24}O_8$	429.1549	429.1552	0.7	427.1393	-	-	135.0458; 297.0775; 353.1373	Acetylation + Reduction + Hydroxylation	+	-	-	-
M20	20.56	$C_{21}H_{20}O_7$	385.1287	385.1284	−0.8	383.1131	383.1129	−0.5	135.0462; 285.0777; 311.0534; 339.1212; 367.1175	Hydroxylation	+	-	-	-
M21	21.52	$C_{21}H_{20}O_7$	385.1287	385.1288	0.3	383.1131	383.1128	−0.8	135.0449; 283.0616; 285.0754; 311.0535; 329.0660; 339.1205; 367.1186	Hydroxylation + Demethylation + Methylation	+	-	-	-
M22	21.52	$C_{20}H_{18}O_5$	339.1232	339.1237	1.5	337.1076	337.108	1.2	135.0463; 255.0659; 283.0599	Dehydroxylation	+	-	-	-
M23	21.56	$C_{21}H_{22}O_8$	403.1393	403.1385	−2	401.1236	-	-	135.0455; 283.0590; 311.0560; 339.1238	2Hydroxylation + Reduction	+	-	-	-
M24#	22.42	$C_{23}H_{24}O_7$	413.16	413.1591	−2.2	411.1444	411.1436	−1.9	243.0653; 351.1268; 367.1174; 379.1195	Reduction + Acetylation	+	-	-	-
M25#	22.44	$C_{23}H_{24}O_8$	429.1549	-	-	427.1393	427.1393	0	139.0383; 351.1233; 367.1165; 395.1141	Hydroxylation + Reduction + Acetylation	+	-	-	-

P = plasma; U = urine; B = Bile; F = feces. "–", not detected. "#", MS/MS fragment ions given in table were detected in negative mode.

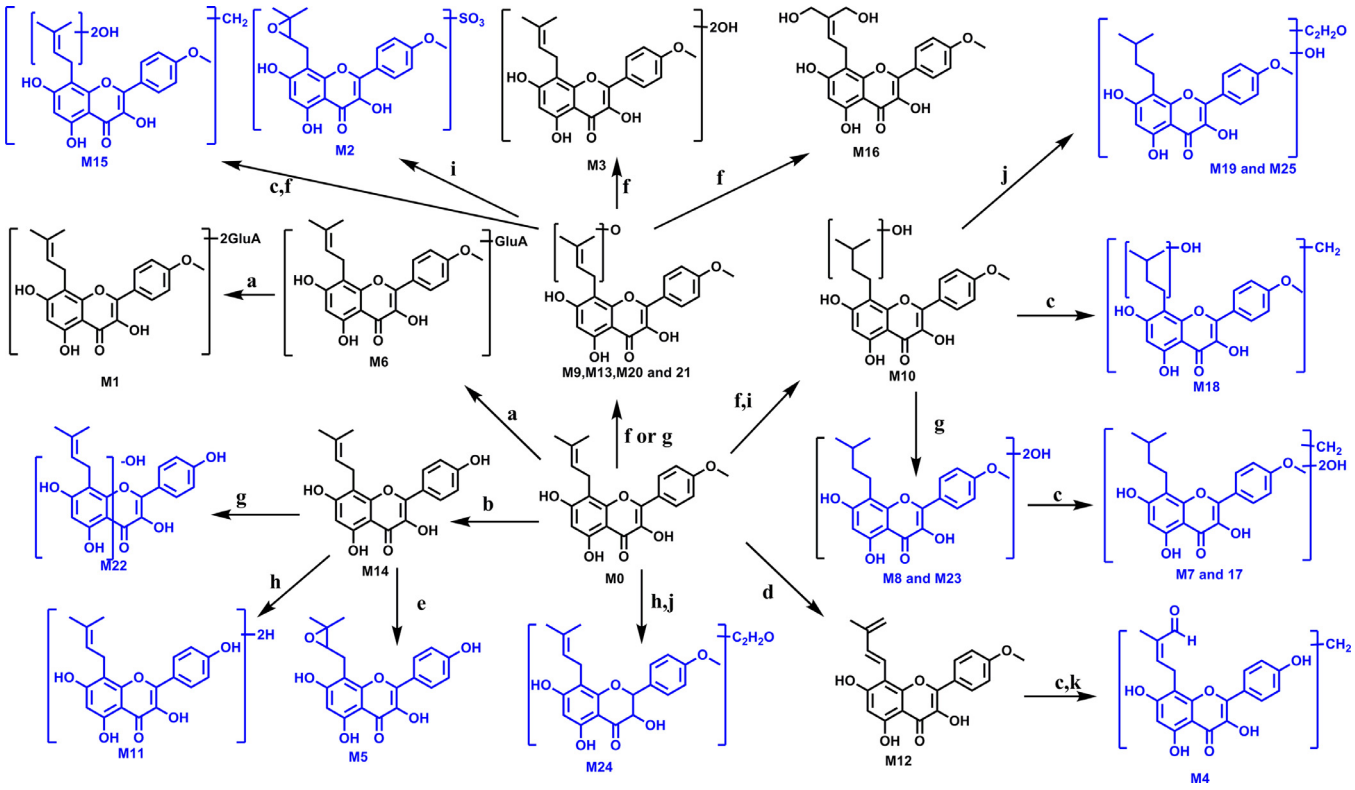

Fig. 3. Proposed fragmentation pathways (a. glucuronide conjugation; b. demethylation; c. methylation; d. dehydrogenation; e. epoxidation; f. hydroxylation; g. dehydroxylation; h. reduction; i. sulfation; j. acetylation; k. oxidation. Metabolites in blue were identified for first time, and metabolites in black were reported before.).

ion at *m/z* 313.0729 indicated that the both oxygens were located at isopentenyl. Referring to the study of J. Jiang (Jiang et al., 2014), it was speculated that dihydroxylation occurred at two methyl of isopentenyl.

M5 was eluted at 12.45 min with the formula ($C_{20}H_{18}O_7$) and deprotonated ion at *m/z* 369.0966 calculated by the Metabolynx software, and the neutral loss of 16 Da (O) can be detected in the MS/MS spectrum. Thus, M5 was speculated as the demethylation metabolite of icaritin with epoxy group at isopentenyl.

M8 and **M23** were eluted at 14.04 min and 21.56 min, respectively. Compared with M3, both the molecular ion at *m/z* 403.1393 and fragment ion at *m/z* 385.1293 of M8 ($C_{21}H_{22}O_8$) were 2 Da more than those of M3 (*m/z* 401.1231, 383.1125), and the neutral loss of 18 Da (H_2O) between the ions *m/z* 403.1389 and 385.1293 and another one between the ions at *m/z* 385.1293 and 367.1152 were detected in the MS/MS spectrum. Based on the fragment ion at *m/z* 313.0718, M8 was diagnosed as the dihydroxylation metabolite of icaritin and the reduction occurred at isopentenyl. M23 was the isomer of M8 and the fragment ion at *m/z* 311.0560 indicated that the dihydroxylation and reduction also occurred at isopentenyl, while the position of hydroxyl cannot be confirmed.

M9, M13, M20 and **M21,** with the same formula ($C_{21}H_{20}O_7$), were eluted at 14.06, 15.53, 20.56 and 21.52 min, respectively. Based on the fragment ion at *m/z* 311.0535 of M13, M20 and M21 and the fragment ion at *m/z* 285.0761 of M9, M20 and M21, the extra oxygen of the four metabolites compared with M0 was located at the isopentenyl. While, whether hydroxylation and epoxidation occurred remain uncertain.

M10 ($C_{21}H_{22}O_7$) was eluted at 15.46 min with the molecular ion at *m/z* 387.1436 and fragment ion at *m/z* 369.1335 which were 2 Da more than those of M9 (*m/z* 385.1285, 367.1182). Based on the fragment ion at *m/z* 313.0714, it was confirmed that the reduction was occurred at the double bond of isopentenyl while the position of hydroxyl was uncertain.

3.3. Dehydrogenation metabolite of icaritin

M12 ($C_{21}H_{18}O_6$) was eluted at 15.53 min with the molecular ion at *m/z* 367.1183 which was 2 Da less than that of M0. Thus, M12 was diagnosed as the dehydrogenation metabolite of icaritin, which was also reported by Zhang BB and coworkers (Zhang et al., 2017).

3.4. Methylation metabolites of icaritin

M7 ($C_{22}H_{24}O_8$) and **M17** were eluted at 13.35 and 16.40 min, respectively, and were a pair of isomers with the deprotonated ion at *m/z* 415.1396 in the negative mode which were 48 Da (CH_4O) more than that of M0 based on the formula supported by Metabolynx software. Methylation, reduction and dihydroxylation were metabolite types calculated by Metabolynx, based on the common fragment ion at *m/z* 311.0573, it was speculated that the reduction was occurred at isopentenyl, while the position of methyl and hydroxyl remain uncertain.

M15 ($C_{22}H_{22}O_8$) was eluted at 16.11 min with the molecular ion at *m/z* 415.1394 and fragment ion at *m/z* 383.1099 in the positive mode were same as that of M17 (*m/z* 415.1396, 383.1162) in the negative mode, which indicated that M15 was the methylation and dihydroxylation metabolite of icaritin without reduction compared with M17.

With the same fragment ions of M10 at *m/z* 313.0707 and 369.1331, **M18** ($C_{22}H_{24}O_7$) was eluted at 18.75 min. The molecular ion of M18 was at m/z 401.1606, 14 Da more than that of M10 which indicated that methylation occurred at some inconclusive position of M18 on the basis of the same metabolite type of M10 (hydroxylation and reduction).

M4 ($C_{22}H_{18}O_7$) was eluted at 12.24 min with the molecular ion at *m/z* 395.1124. The fragment ions of M4 at *m/z* 297.0782 and 325.0715 were 14 Da more than that of M12 at m/z 283.0607 and

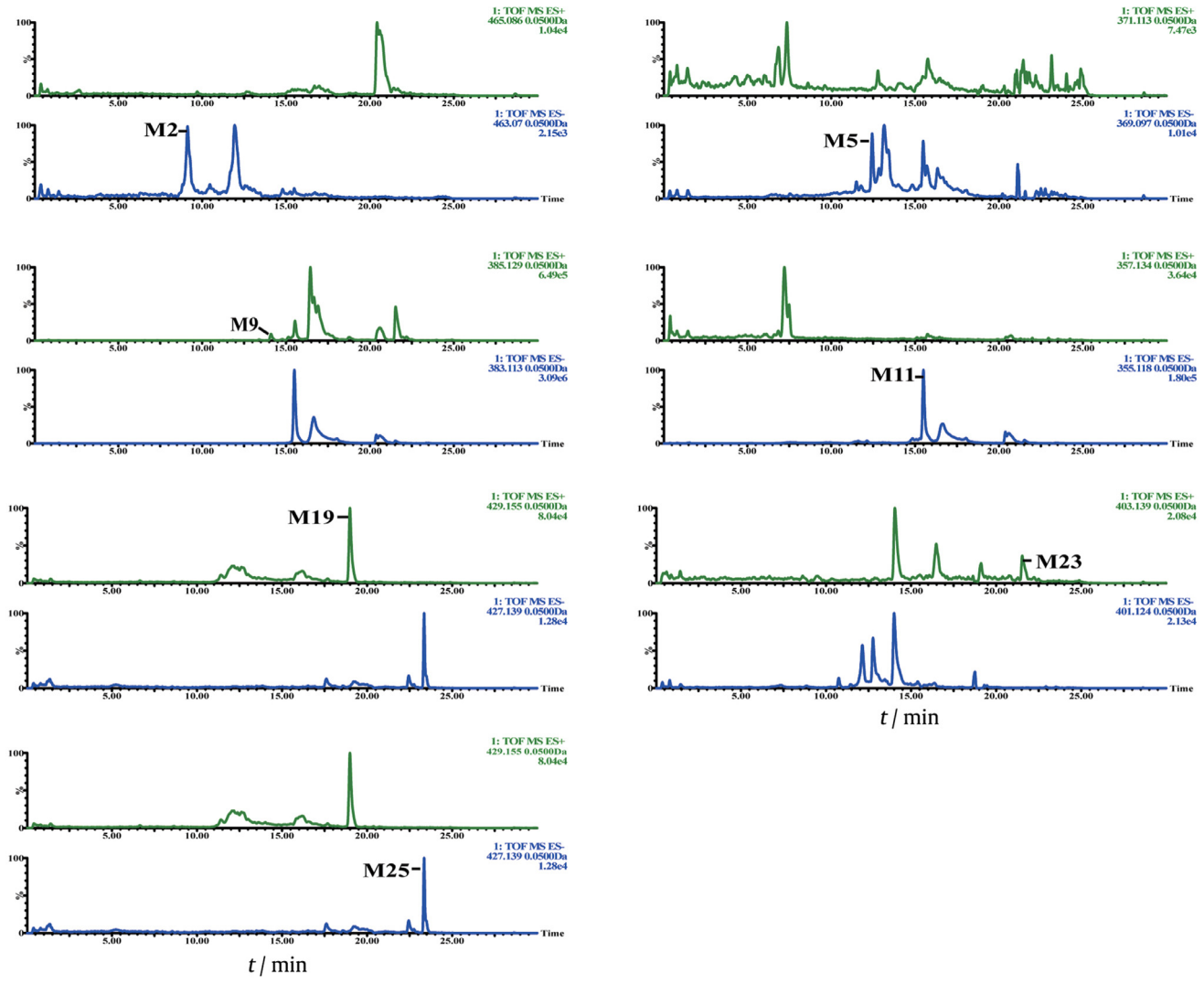

Fig. 4. Comparisons of typical metabolites in positive and negative modes.

311.0563 which indicated that there was an extra methyl on fragments of M4 compared with M12. However, there were 28 Da (CO) and one more degree of unsaturation of M4 than M12 based on the formula calculated by Metabolynx software. Thus, it was speculated that the methyl of isopentenyl was oxidized into formyl.

3.5. Acetylation metabolites of icaritin

M19 ($C_{23}H_{24}O_8$) and **M25** were eluted at 18.98 and 22.44 min, respectively. Based on the formula calculated by Metabolynx software, there was extra C_2H_2O compared with M10. Thus, it was speculated that acetylation occurred at some position of M19 and M25 based on the structure of M10.

With extra C_2H_4O than M0, **M24** ($C_{23}H_{24}O_7$) was eluted at *m/z* 22.42 min. The fragment ion with one more degree of unsaturation at *m/z* 379.1195 was 32 Da (M24-CH_2-H_2O) less than M24, which indicated that the double bond on C-ring of M24 was saturated. It was speculated that M24 was acetylation and reduction metabolite of icaritin.

3.6. Demethylation metabolites of icaritin

M14 ($C_{20}H_{18}O_6$) was eluted at 15.74 min with the molecular ion at *m/z* 355.1181 which was 14 Da (CH_2) less than that of M0. Therefore, M14 was diagnosed as demethylation metabolite of icaritin.

The molecular ion and fragment ion of **M22** ($C_{20}H_{18}O_5$) at *m/z* 339.1237 and 283.0599 were both attributed to the loss of 16 Da relative to the ions of M14 (*m/z* 355.1181 and 299.0549). The fragment ion at *m/z* 135.0463 indicated that the B-ring was unaltered. All together, in consideration of the intramolecular hydrogen bond, the hydroxyl on C-5 was more steady. Thus, it was speculated that the dehydroxylation occurred on C-6.

3.7. Reduction metabolite of icaritin

The deprotonated ion of **M11** ($C_{20}H_{20}O_6$) at *m/z* 355.1177 was 2 Da more that of M14 at *m/z* 353.1022 which indicated that reduction occurred at some position of M11 based on the structure of M10.

4. Discussion

In the present study, an UPLC/Q-TOF-MS/MS method was established for the identification of *in vivo* metabolites of icaritin in rats after three consecutive days of orally administration at the dose of 100 mg/kg. The identification of metabolites is usually confusing owing to various possibilities of metabolite types. With the aid of

the Metabolynx software, setting the expectant metabolite types in the software beforehand, and then making a contrast between biosamples of experimental group and control group, the potential metabolites and corresponding metabolite types were provided. And the acetylation metabolites detected in this study were identified in this way. Based on the valuable information offered by the Metabolynx software and the accurate mass measurements, MS^2 fragmentation patterns, chromatographic retention time, and the structures of metabolites were characterized more exact and easier.

The formation of these metabolites can be attributed to glucuronide conjugation, demethylation, methylation, dehydrogenation, epoxidation, hydroxylation, dihydroxylation, reduction, sulfation, oxidation, and acetylation. It was summarized as following: 1. methoxyl on the ring-B was apt to demethylate; 2. olefinic bond of isopentene group was susceptible to occur reduction biotransformation; 3. isopentenyl was a sensitive group which was prone to occur hydroxylation, epoxidation, reduction, and oxidation; 4. Hydroxylation, acetylation, and methylation were significant biotransformations; These observations indicated that icaritin underwent extensive metabolism which perhaps can be responsible for the low bioavailability. The proposed metabolic fates were shown in Fig. 3. Although there have been four articles available concerning the metabolism of icaritin (Jiang et al., 2014; Ye et al., 2015; Zhang et al., 2017; Zhang & Zhang, 2017), the acetylation metabolites were unnoticed. Acetylation is an uncommon metabolite type of flavonoid but not impossible. As far as know, the acetylation occurred in the study of *in vivo* (Du et al., 2015) and *in vitro* metabolites of flavonoids (Tao, Duan, Jiang, Qian, & Qian, 2016a; Tao, Duan, Qian, Qian, & Guo, 2016b; Xue et al., 2011). Thus, it is necessary to pay attention to the acetylation in the study of metabolites of flavonoids.

To make the results more comprehensive, the detection of metabolites were conducted in both positive and negative modes of UHPLC/Q-TOF-MS/MS. **M9, M19,** and **M23** were more suitable for the positive mode, while **M2, M5, M11,** and **M25** had better response in the negative mode. Some typical metabolites were illustrated in Fig. 4. This phenomenon enlightens us that it is possible to neglect some significant signals as detecting biosamples in the single ion test mode. While the relationship between the structure of metabolites and corresponding response requires further study.

5. Conclusion

With the analysis of both positive and negative modes, a total of 25 metabolites were detected, including 24 metabolites in feces, three metabolites in bile, four metabolites in urine and one metabolites in plasma, and 14 of them were reported for the first time. Hydroxylation, methylation, and acetylation were the main phase I metabolite types, meanwhile, glucuronide conjugation and sulfation were diagnosed as phase II metabolites. This research provides scientific and reliable support for full understanding of the metabolism of icaritin, which is a valuable candidate compound of clinical therapy for several kinds of diseases.

Conflict of interest

All authors declare no conflict of interest.

Acknowledgment

This work was supported by the National Natural Science Foundation of China (NSFC) [No. 81430095].

References

Du, L. Y., Qian, D. W., Shang, E. X., Liu, P., Jiang, S., Guo, J. M., et al. (2015). UPLC-Q-TOF/MS-based screening and identification of the main flavonoids and their metabolites in rat bile, urine and feces after oral administration of *Scutellaria baicalensis* extract. *Journal of Ethnopharmacology, 169*, 156–162.

Feng, X. C., Huo, X. G., Liu, H. X., Chai, L. W., Ding, L. Q., & Qiu, F. (2017). Identification of absorbed constituents and *in vivo* metabolites in rats afteroral administration of *Physalis alkekengi* var. *franchetii* byultrahigh-pressure liquid chromatography quadrupole time-of-flight massspectrometry. *Biomedical Chromatography, 177*(3), 44–55.

Jiang, J., Feng, L., Sun, E., Li, H. T., Cui, L., & Jia, X. B. (2014). Metabolic profiling of isomeric aglycones central-icaritin (c-IT) and icaritin (IT) in osteoporotic rats by UPLC-QTOF-MS. *Drug Testing and Analysis, 7*(4), 309–319.

Jiang, J., Zhao, B. J., Song, J., & Jia, X. B. (2016a). Pharmacology and clinical application of plants in *Epimedium* L. *Chinese Herbal Medicines, 8*(1), 12–23.

Jiang, M. C., Chen, X. H., Zhao, X., Zhang, X. J., & Chen, W. F. (2016b). Involvement of IGF-1 receptor signaling pathway in the neuroprotective effects of Icaritin against MPP+- induced toxicity in MES23.5 cells. *European Journal of Pharmacology, 786*, 53–59.

Kim, D. H., Jung, H. A., Sohn, H. S., Kim, J. W., & Choi, J. S. (2017). Potential of icariin metabolites from *Epimedium koreanum* Nakai as antidiabetic therapeutic agents. *Molecules, 22*(6), 986 986/1-986/14.

Li, J., Liu, P., Zhang, R. X., Cao, L., Qian, H. H., Liao, J., et al. (2011). Icaritin induces cell death in activated hepatic stellate cells through mitochondrial activated apoptosis and ameliorates the development of liver fibrosis in rats. *Journal of Ethnopharmacology, 137*(1), 714–723.

Li, Q. H., Huai, L., Zhang, C. P., Wang, C. C., Jia, Y. J., Chen, Y. R., et al. (2013). Icaritin induces AML cell apoptosis via the MAPK/ERK and PI3K/AKT signal pathways. *International Journal of Hematology, 97*(5), 617–623.

Liu, H. P., Meng, F. H., Guo, J. F., Si, D. Y., Zhu, X. W., & Zhao, Y. M. (2010). Pharmacokinetics of icaritin in rats. *Chinese Pharmaceutical Journal, 45*(7), 539–543.

Sun, C. H., Pan, L. H., Yang, J., Yao, J. C., Li, B. B., Tan, Y. J., et al. (2018). Protective effect of icaritin on focal cerebral ischemic-reperfusion mice. *Chinese Herbal Medicine, 10*(1), 40–45.

Sun, F., Zhang, Z. W., Tan, E. M., Lim, Z. L. R., Li, Y., Wang, X. C., et al. (2016). Icaritin suppresses development of neuroendocrine differentiation of prostate cancer through inhibition of IL-6/STAT3 and Aurora kinase A pathways in TRAMP-mice. *Carcinogenesis, 37*(7), 701–711.

Tan, E. M., Li, L., Indran, I. R., Chew, N., & Yong, E. L. (2017). TRAF6 Mediates suppression of osteoclastogenesis and prevention of ovariectomy-induced bone loss by a novel prenylflavonoid. *Journal of Bone and Mineral Research, 32*(4), 846–860.

Tao, J. H., Duan, J. A., Jiang, S., Qian, Y. Y., & Qian, D. W. (2016a). Biotransformation and metabolic profile of buddleoside with human intestinal microflora by ultrahigh-performance liquid chromatography coupled to hybrid linear ion trap/orbitrap mass spectrometer. *Journal of Chromatography B, 1025*, 7–15.

Tao, J. H., Duan, J. A., Qian, Y. Y., Qian, D. W., & Guo, J. M. (2016b). Investigation of the interactions between *Chrysanthemum morifolium* flowers extract and intestinal bacteria from human and rat. *Biomedical Chromatography, 30*(11), 1807–1819.

Wang, J., Chen, H., Mai, D. N., Ma, H. R., Wang, Z. H., & Li, Y. (2013). Effects of icariin and icaritin on proliferation of breast cancer T47D cells. *Chinese Traditional and Herbal Drugs, 44*(11), 1470–1475.

Wang, Y., Yuan, L., Li, Y. B., & Zhang, Y. J. (2017). Analysis on chemical constituents of *Epimedii Folium* by UPLC-Q-TOF-MS. *Chinese Traditional and Herbal Drugs, 48*(13), 2625–2631.

Wu, T., Shu, T., Kang, L., Wu, J. H., Xing, J. Z., Lu, Z. Q., et al. (2017). Icaritin, a novel plant-derived osteoinductive agent, enhances the osteogenic differentiation of human bone marrow- and human adipose tissue-derived mesenchymal stem cells. *International Journal of Molecular Medicine, 39*(4), 984–992.

Xu, B., Jiang, C. W., Han, H. X., Liu, H., Tang, M., Liu, L. X., et al. (2015). Icaritin inhibits the invasion and epithelial-to-mesenchymal transition of glioblastoma cells by targeting EMMPRIN via PTEN/AKt/HIF-1a signaling. *Clinical and Experimental Pharmacology & Physiology, 42*(12), 1296–1307.

Xue, C. F., Jiang, S., Guo, J. M., Qian, D. W., Duan, J. A., & Shang, E. X. (2011). Screening for *in vitro* metabolites of *Abelmoschus manihot* extract in intestinal bacteria by ultra-performance liquid chromatography/quadrupole time-of-flight mass spectrometry. *Journal of Chromatography B, 879*(32), 3901–3908.

Yao, D., Xie, X. H., Wang, X. L., Wan, C., Lee, Yuk-Wai, Chen, S. H., et al. (2012). Icaritin, an exogenous phytomolecule, enhances osteogenesis but not angiogenesis—an *in vitro* efficacy study. *PLoS One, 7*(8), E41264.

Ye, L. H., Xiao, B. X., Cao, F. R., Zhang, Y., Pan, R. L., & Chang, Q. (2015). Identification of icaritin metabolites in rats by LC-MS/MS. *Chinese Herbal Medicines, 7*(4), 296–302.

Zhang, B. B., Chen, X. L., Zhang, R., Zheng, F. F., Du, S. Z., & Zhang, X. J. (2017). Metabolite profiling, pharmacokinetics, and *in vitro* glucuronidation of icaritin in rats by ultra-performance liquid chromatography coupled with mass spectrometry. *Journal of Analytical Methods in Chemistry, 2017*, 1–13 1073607/1-1073607/13.

Zhang, S. Q., & Zhang, S. Z. (2017). Oral absorption, distribution, metabolism, and excretion of icaritin in rats by Q-TOF and UHPLC-MS/MS. *Drug Testing and Analysis, 9*(10), 1604–1610.